Society For Biomaterials

pH-dependent immobilization of urease on glutathione-capped gold nanoparticles

Seema Garg,[1] Arnab De,[2] Subho Mozumdar[1]

[1]Department of Chemistry, University of Delhi, Delhi 110007, India
[2]Department of Microbiology and Immunology, Columbia University, New York City, New York

Received 7 July 2014; accepted 6 August 2014
Published online 00 Month 2014 in Wiley Online Library (wileyonlinelibrary.com). DOI: 10.1002/jbm.a.35314

Abstract: Urease is a nickel-dependent metalloenzyme that catalyzes the hydrolysis of urea to form ammonia and carbon dioxide. Although the enzyme serves a significant role in several detoxification and analytical processes, its usability is restricted due to high cost, availability in small amounts, instability, and a limited possibility of economic recovery from a reaction mixture. Hence, there is a need to develop an efficient, simple, and reliable immobilization strategy for the enzyme. In this study, the carboxyl terminated surface of glutathione-capped gold nanoparticles have been utilized as a solid support for the covalent attachment of urease. The immobilization has been carried out at different pH conditions so as to elucidate its effect on the immobilization efficiency and enzyme bioactivity. The binding of the enzyme has been quantitatively and qualitatively analyzed through techniques like ultraviolet–visible spectroscopy, intrinsic steady state fluorescence, and circular dichorism. The bioactivity of the immobilized enzyme was investigated with respect to the native enzyme under different thermal conditions. Recyclability and shelf life studies of the immobilized enzyme have also been carried out. Results reveal that the immobilization is most effective at pH of 7.4 followed by that in an acidic medium and is least in alkaline environment. The immobilized enzyme also exhibits enhance activity in comparison to the native form at physiological temperature. The immobilized urease (on gold glutathione nanoconjugates surface) can be effectively employed for biosensor fabrication, immunoassays and as an *in vivo* diagnostic tool in the future.

Key Words: glutathione, gold nanoparticles, urease, covalent immobilization

How to cite this article: Garg S, De A, Mozumdar S. 2014. pH-dependent immobilization of urease on glutathione-capped gold nanoparticles. J Biomed Mater Res Part A 2014:00A:000–000.

INTRODUCTION

While, in general, the loss of protein secondary structure and consequent changes in its activity upon interactions with nanomaterials can be seen as a potential source of nanoparticle toxicity, there exists a budding positive outcome too. Promising applications of nanoparticle–protein interactions include increasing protein stability toward enzyme degradation and enhancing activity (if any) and stability of enzyme in aqueous and non-aqueous media via immobilization at surfaces.[1] Enzyme immobilization has specifically attracted interest due to the convenience in handling, ease of separation of enzymes from the reaction mixture and reuse, low product cost, and a possible increase in thermal and pH stability along with an increase in the overall bioactivity of the immobilized enzyme in a few cases.[2–5]

A wide variety of immobilization techniques have been employed including adsorption on solid supports,[6,7] covalent attachment,[8,9] or entrapment in silica/polymer matrices.[10] The techniques involving physical bonding are usually very easy to apply, but suffers from major shortcomings such as leaching of the enzyme with subsequent conformational changes due to weak binding.[11,12] Covalent attachment, on the other hand, can lead to improved enzyme stability, often *in lieu* of the partial inactivation of enzyme due to the conformational changes induced by the covalent bonding of the enzyme residues to the nanostructure.[13] It has been observed that in certain cases, the immobilization can induce structural [three-dimensional (3D)] changes which might affect the entire molecule. Thus, an essential requirement for a successful immobilization lies in the selection of an appropriate surface/matrix that should provide a biocompatible/inert environment and should not interfere with the active site of the enzyme (resulting in its compromised biological activity).[14]

Gold nanoparticles, in this context, have emerged as an excellent immobilization surfaces owing to their inertness, non-toxicity, and non-immunogenicity together with extreme surface activity and modification flexibilities. Several research groups have directly immobilized enzymes on to bare nanogold surfaces (without any modification) through the very well-known gold-thiol chemistry.[15–17] Apart from

Correspondence to: S. Mozumdar; e-mail: subhoscom@yahoo.co.in

this, the surface of the gold nanoparticles can also be easily and efficiently functionalized with thiolated molecules and carboxylic groups, which in turn, can be conjugated with amino groups of the proteins and/or enzymes.[18–21]

Urease (urea amidohydrolase, EC 3.5.1.5) is a highly efficient enzyme for converting urea to ammonia and carbon dioxide.[22] It plays a crucial role in the determination of urea in blood, urine, and wastewater and can hence contribute significantly in the process of dialysis (for removal of urea from blood in the treatment of uremia).[23] Moreover, the enzyme is found in a variety of bacteria, fungi, and plants, thus playing an important role in the circulation of nitrogen in nature.[24] However, the usability of the enzyme suffers from some major constraints such as its post analysis separation from the reaction mixture, storage, unavailability, and its working efficiency at high temperature (60°C). As a consequence, there exists an inevitable quest for the development of an appropriate immobilization strategy for this enzyme.

Many polymeric materials have been utilized as the immobilization surface till now.[23,25–28] Materials such as calcium alginate gel spheres, lac impregnated muslin cloth, and paraffin wax impregnated muslin cloth have also been used.[29] Immobilization on the mentioned materials, however, either involved tedious/harsh immobilization methods or resulted in compromised enzyme activity (due to leaching and inactivation of active site). Recently, phosphonated iron oxide nanoparticles have also been employed as the effective immobilization surface for urease.[24] Although they broadened the pH and thermal stability range of the enzyme but again resulted in compromised enzyme activity with 57% specific bioactivity retained.

Hence, in view of the phenomenal advantages presented by the inert, non-toxic, and chemically reactive surface of gold nanoparticles, an attempt to covalently immobilize urease on to the surface of the glutathione-capped gold nanoparticles has been made and discussed in this article. The immobilization has been attempted under acidic (pH 4.0), neutral (pH 7.4), and alkaline (pH 9.2) conditions. The study is intended toward the evaluation of benefits offered by the gold-glutathione nanoconjugates as the promising surface for the enzyme immobilization.

MATERIALS AND METHODS

Materials

All starting materials were purchased from commercial sources and were used without further purification. Specifically, gold chloride (49%–50% Au; $HAuCl_4$) was procured from Merck (Germany). Glutathione and urease was a product of Sigma (United States). EDC and NHS were again purchased from Merck (India). Chemical used for the buffer preparations were of analytical grade (AR) and were procured from SRL (Mumbai, India). Urea, EDTA, and sodium tungstate were obtained from Fischer Scientifics (Mumbai, INDIA). Double distilled water was used throughout the experiments and was produced in the laboratory (WDU 2000). Cold temperature was maintained in an ice bath whereas elevated temperatures were maintained in a thermostable water bath.

The Fourier transform infrared (FT-IR) data was obtained on a Perkin-Elmer, FTIR-1710 spectrophotometer. Ultraviolet (UV) analysis for the samples was done on Double beam Systronics AU2700 instrument. Fluorescence studies were conducted on a CARY instrument with an excitation value of 280 nm. The dynamic light scattering (DLS) measurements for estimating the average mean size and polydispersity index were carried out on a Photocor FC instrument having Argon ion laser (633 nm) as the light source and Dyna LS as the software for accumulating data points and plotting a diffractogram. TEM Micrographs were collected from TECHNAI ULTRA TWIN FEI with EDAX instrument operating at an applied voltage of 300 kV. Circular dichorism (CD) studies were conducted in the far UV region (from 190 to 300 nm) at room temperature on a JASCO J-810 spectrometer (JASCO Spectroscopic Co., Hachioji, Japan). Secondary structure content was calculated using the program CONTIN. Denver analytical weighing balance was used for the gravimetric analysis.

Methods

Synthesis of gold-glutathione nanoconjugates. Gold-glutathione nanoconjugate was synthesized employing the reverse micellar template of a biocompatible non-ionic surfactant in a non-aqueous medium. Briefly, 54 μL of 0.05*M* aqueous solution of gold chloride was added to 10 mL of the stock surfactant solution so as to form reverse micelle A (RM-A). Similarly, in another 10ml of the stock surfactant solution, 54 μL of the 0.25*M* aqueous solution of sodium borohydride was added to form reverse micelle-B (RM-B). Both RM-A and RM-B were equilibrated under constant magnetic stirring for about 20–25 minutes before RM-B was added to RM-A dropwise to form a homogeneous mixture (RM-C). Immediately after the addition of the content of RM-B to RM-A, 36 μL of 5 m*M* glutathione was added to the resultant RM-C. RM-C was then left on magnetic stirring for another 3 h. Finally the micelles were disrupted using 2–3 mL of benzene:methanol (3:1) solvent mixture. The disrupted micelles were centrifuged at 3000—4000 rpm for 8–10 minutes so as to collect the suspended particles. The particles were washed thoroughly with absolute ethanol in order to remove the impurities of synthetic precursors such as surfactant residue, unreacted ions, etc. The concentrated particle suspension was then air-dried for its further characterization and derivatization.

In vitro cytotoxicity assessment of gold glutathione nanoconjugates. The cytocompatibility studies of the glutathione conjugated and bare gold nanoparticles were carried out on A549 human cell lines via MTT cell viability assay. Human alveolar basal epithelial (A549) cells were cultured in Dulbecco's modified Eagle's medium (DMEM) supplemented with 10% fetal bovine serum (Invitrogen) and 1% antibiotic (Sigma). The cells were maintained at 37°C in a 5% CO_2 incubator. Approximately, 1×10^5 cells were plated in 96 well plates. Various concentrations of the bare and

conjugated gold nanoparticles were then prepared via serial dilution method from a stock solution of 100 μg/mL. The concentrations of the gold samples so obtained were 100, 50, 25, 12.5, 6.25, 3.125, and 1.56 μg/mL. Each concentration was assessed in triplicates. In other words, each concentration of the bare and conjugated gold nanoparticles was added in triplicates to the A549 cells. Following the addition of gold samples, the cells were incubated at 37°C in 5% CO_2 incubator for 24 h. After incubation, 20 μL of MTT reagent (Sigma) was added to each well and was again incubated for 3 h at 37°C. Finally, the MTT reagent was removed and 100 μL of DMSO (solubilization solution) was added in each well. The plate was then kept for vigorous shaking for about 15 minutes with the subsequent measurement of the optical density (of cells) at 570 nm.

EDC–NHS derivatization of gold glutathione nanoconjugates. Derivatization of the surface exposed carboxyl moiety of the gold-glutathione nanoconjugate involved the addition of EDC.hydrochloride (20 mg; dissolved in 1 mL of the phosphate buffer at pH 7.4) to 5 mL of the conjugated gold colloid (at a concentration of 1000 ppm in the phosphate buffer 7.4). The temperature during the addition was maintained between 0°C and 4°C. The reaction mixture was then incubated at the same temperature for about an hour with the magnetic stirring turned on. Following this, 20 mg of NHS again dissolved in 1 mL of the phosphate buffer (pH 7.4) was added to the reaction mixture. The reaction mixture was finally incubated for another 1 h maintaining the same conditions of temperature. The red colored colloid thus formed was centrifuged at 8000–10,000 rpm for about 8–10 minutes so as to separate the activated glutathione-capped gold nanoparticles from the unreacted precursors. The pellet was washed with double distilled water and was air dried for the further studies. For the storage purposes, the activated gold glutathione nanoconjugate was kept at 0°C–4°C.

Immobilization of* urease *on the surface of the gold glutathione nanoconjugates at different pH values. A typical procedure employed for the immobilization of urease on the surface of the activated gold glutathione nanoconjugate is discussed as follows:—Pre-weighed amount of absolutely dried activated gold-glutathione nanoconjugate (2 mg) was dispersed in 2 mL of the buffer (at pH 4.0, pH 7.4, and pH 9.2 separately) under mild sonication conditions. Each of the well-dispersed gold colloid so obtained (i.e., at pH 4.0, 7.4, and 9.2) was incubated at a temperature of 0°C–4°C for about 10–15 minutes before 3 mL of the urease suspension (1.33 mg/mL; prepared in the respective buffers) was added to them. The resultant suspensions containing enzyme and gold colloid in the ratio of about 2:1 at different pH values of 4.0, 7.4, and 9.2, were incubated at the maintained temperature of 0°C–4°C for about 2 h followed by their incubation at room temperature for 12 h. The urease bound gold nanoparticles were then separated from the free unbound enzyme through centrifugation at 8000–10,000 rpm for 10 minutes. The supernatant was collected separately and subsequently labeled. The pellets of the urease bound gold nanoparticles thus obtained were washed slightly with double distilled water and redispersed in the 5 mL of their respective buffers. Final nanoparticulate suspensions containing the immobilized urease were designated as IM.U.4, IM.U.7, and IM.U.9 depending upon the buffer used and were evaluated for their various physicochemical and binding aspects.

Bioactivity studies of the free as well as* urease *nanoparticulate suspensions. Bioactivity studies of the free and urease nanoparticulate suspensions were carried out as per the procedures given by Krishnan et al.[30] with slight modifications. Briefly, 500 μL of free (40 ppm) or immobilized (1000 ppm) urease dispersed in the assay buffers at different pH values of pH 4.0, 7.4, and 9.2 was taken in separate test tubes such that six test tubes (three for free urease and three for immobilized urease at pH 4.0, 7.4, and 9.2, respectively) were obtained in total. To each of the test tubes, 1.0 mL of respective assay buffer containing 150 m*M* urea and 5 m*M* EDTA was added and incubated at 60°C for 30 minutes. After incubation, 0.3 mL of 0.3% sodium tungstate and 0.3 mL of 0.68*N* sulfuric acid was added to all the test tubes containing free enzyme. However, for the test tubes containing urease nanoparticulate suspension, centrifugation of the enzyme-bound gold nanoparticles was carried out prior to the above mentioned additions. Finally the total volume in each of the test tube was made up to 5 mL using the assay buffer. About 1 mL of the solution so obtained was then taken out and was treated with 1 mL of the Nessler's reagent. The brown colored precipitate thus formed was quantified gravimetrically in order to determine the percentage bioactivity.

Effect of different thermal conditions on the activity of the enzyme was analyzed by carrying out the same procedure at incubation temperature of 0°C, 25°C, and 37°C separately.

Recyclability studies of* urease *nanoparticulate suspension. The urease nanoparticulate suspension IM.U.7 obtained after centrifugation during the bioactivity studies was analyzed four to five times for its activity toward the hydrolysis of urea at the incubation temperature of 37°C and 60°C using the same procedure as mentioned above for analyzing bioactivity.

Shelf-life studies of* urease *nanoparticulate suspension. The urease nanoparticulate suspension IM.U.7 was stored at cold temperature for 90 days. The percentage bioactivity was measured at regular time intervals using the same procedure as mentioned above for the bioactivity analysis at an incubation temperature of 37°C and 60°C individually.

RESULTS AND DISCUSSION

Gold-glutathione nanoconjugates have been employed as a solid surface for the immobilization of enzyme urease in the present study. Immobilization was attempted and quantified at

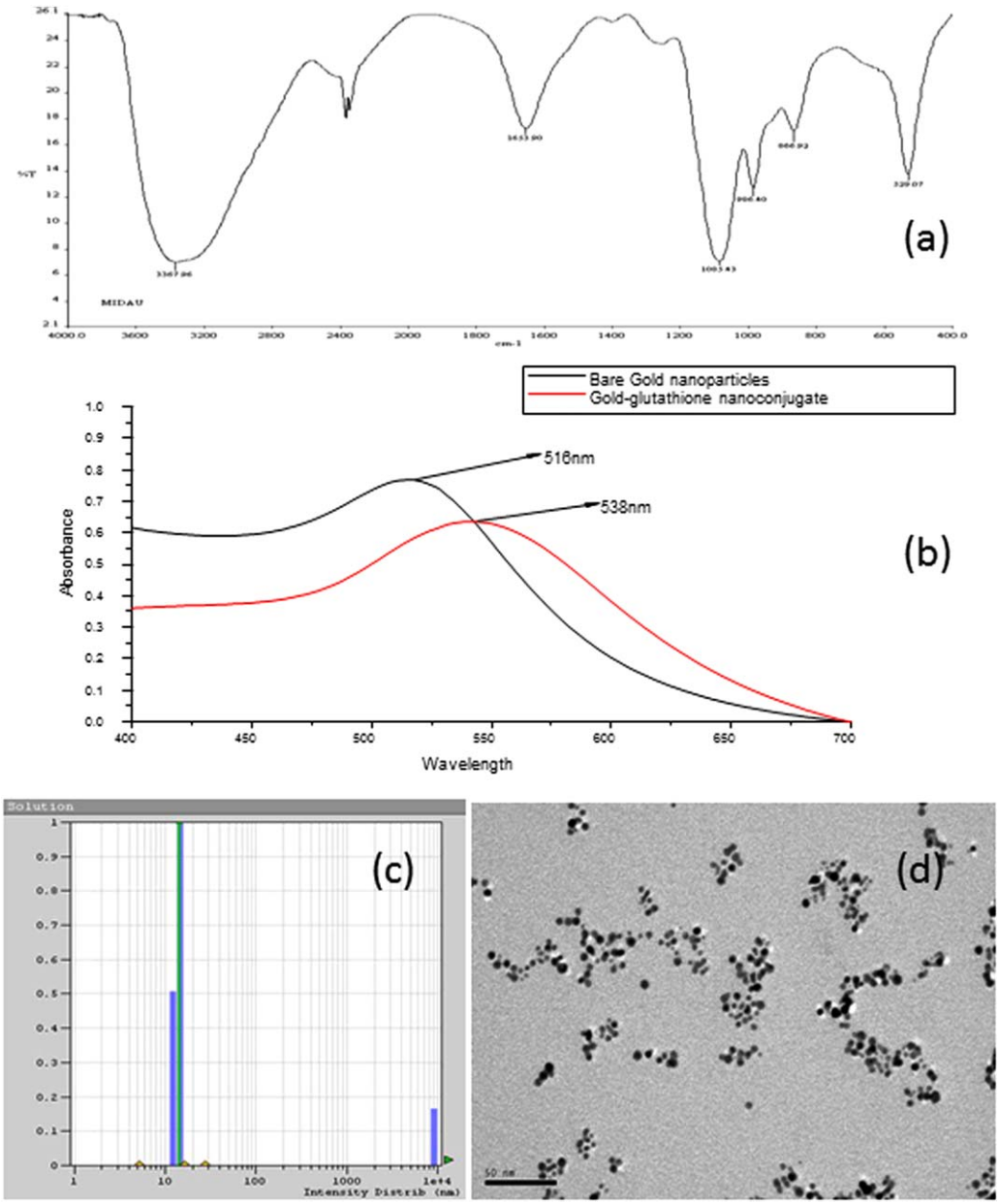

FIGURE 1. Characterization data of gold-glutathione nano-conjugate (a) FT-IR spectrum (b) UV-Vis absorption spectrum (c) Size distribution data (QELS data) (d) TEM micrograph. [Color figure can be viewed in the online issue, which is available at wileyonlinelibrary.com.]

different pH values so as to elucidate the effect of pH on the nature and conformation of the immobilized enzyme. The bioactivity of the immobilized enzyme was then measured gravimetrically with respect to (w.r.t) native enzyme at different pH and temperatures through the signature reaction of urease catalyzed hydrolysis of urea. Finally, the recyclability and shelf life of the immobilized urease has also been enumerated. The results of all the interrelated studies undertaken to accomplish the work objective are discussed sequentially in this section.

Synthesis of gold-glutathione nanoconjugates

Gold-glutathione nanoconjugates were synthesized utilizing the reverse micellar template of a non-ionic surfactant with the capping agent (glutathione) being added after the nucleation of gold nanoparticles. Successful surface functionalization of the gold nanoparticles with glutathione was analyzed through techniques like FT-IR, UV–Vis spectroscopy, and Zeta potential measurements. The physicochemicals aspects of the nanoconjugates were also observed using DLS and transmission electron microscopy (TEM) characterization techniques.

FT-IR spectrum of the nanoconjugates [Fig. 1(a)] shows a distinct and characteristic peak for the vibrational stretching of hydroxyl (—OH) and carbonyl (>C═O) groups at 3350 cm^{-1} and 1650 cm^{-1}, respectively. The peak arising due to the vibrational stretching of ether linkage (C—O)

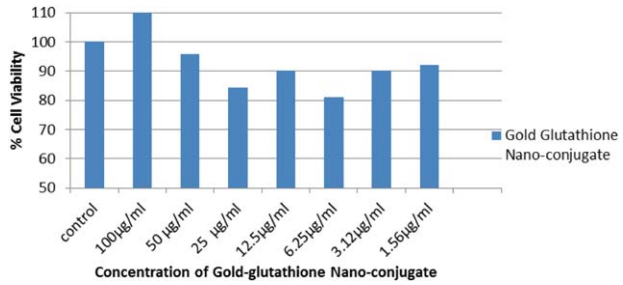

FIGURE 2. A graphical plot of percentage cell viability of A549 cells at different concentrations of gold-glutathione nano-conjugate. [Color figure can be viewed in the online issue, which is available at wileyonlinelibrary.com.]

could also be observed at 1080 cm^{-1}. In the UV–Vis spectrum [Fig. 1(b)], a bathochromic shift in the λ_{max} value from 516 nm (for bare gold nanoparticles) to 538 nm was observed. Furthermore, the measurement of zeta potential of the synthesized nanoconjugate revealed the presence of a negative charge on the nanoconjugate surface with a magnitude of about −35 mV. The results obtained clearly directed toward a successful capping of the gold nanoparticles with glutathione, such that the carboxyl moieties of the latter are surface exposed. The physicochemical analyses of the nanoconjugates [Fig. 1(c,d)] indicate the formation of highly monodispersed spheres of glutathione functionalized gold nanoparticles with a size distribution in the range of 10 ± 5 nm.

In vitro cytotoxicity assessment of gold-glutathione nanoconjugates

In vitro cytotoxicity assessment of the gold-glutathione nanoconjugates on human cell lines (A539) depicts that the cells were viable (showing percentage cell viability of 80% and above) at all the concentrations ranging from 100 to 1.56 μg/mL (Fig. 2).

Hence, they can be safely employed as a solid support for the immobilization of any biologically relevant moiety with its subsequent administration inside the human body.

Immobilization of urease on the surface of gold-glutathione nanoconjugates at different pH values

Urease was covalently immobilized on the surface of the gold-glutathione nanoconjugates through carbadiimide-N-hydroxy succinimide chemistry. The general scheme followed for the immobilization of enzyme on the nanomaterial surface is shown in Scheme 1. The suspensions of the immobilized urease (IM.U.4, IM.U.7, and IM.U.9) were then analyzed for the nature and extent of immobilization (as a function of pH) in a qualitative and quantitative manner through techniques like light scattering and absorption/emission spectroscopy. Conformational behavior of the free and immobilized enzyme was also examined through CD studies.

DLS studies. DLS determines small changes in the hydrodynamic size of particles and can be used to detect the size distribution of nanoparticles. When proteins bind to the nanoparticle surface, size of the latter is presumed to increase.[31]

In this case, DLS data (Fig. 3) indicates a hydrodynamic size of about 100 ± 10 nm for all the three urease nanoparticulate suspensions and this is way higher than the size of the gold-glutathione nanoconjugates [Fig. 1(c)]. Thus, it can be inferred that a successful immobilization of urease occurred on the nanoconjugates surface at all the three pH values. Moreover, as the pH was increased from 4.0 to 9.2, a substantial decrease in the polydispersity of the nanoparticles could be observed. This could be due to the development of negative charge on the surface of urease under basic conditions which led to the effective repulsion amongst the nanoparticles and relatively reduced the protein–protein interactions.[32]

Absorption spectroscopy. Changes in the absorption spectra of the nanoparticle and/or enzyme such as shift in the absorption maxima or broadening of peak can be used to evaluate the binding qualitatively.[31]

In the present study, UV–Vis analysis (Fig. 4) indicates that free urease in the blank reference solution, (irrespective of the pH) shows an absorption maximum at 280 nm.[33] However, upon immobilization, a slight blue shift in the values of λ_{max} (in the range of 268—274 nm) could be observed. In addition, a noticeable blue shift in the λ_{max} value for the gold nanoparticles from 537 nm (for gold-glutathione nanoconjugates) to 532–526 nm (for urease nanoparticulate suspensions: IM.U.4, IM.U.7, and IM.U.9) together with a broadening of peak could be observed. The shift in the λ_{max} value of both the enzyme and the nanoparticles directed toward an affirmative change on the surface of the nanoconjugates in the presence of urease. However, no quantitative information regarding the extent of immobilization and binding affinity at different pH values could be obtained from the UV–Vis absorption studies.

Emission spectroscopy. The alterations in the emission spectra of urease can be used in a more quantitative manner to monitor the changes in the microenvironment of the enzyme upon binding with the nanoconjugates, together with determining the extent of immobilization and efficiency.[31]

Emission spectra of blank reference solutions (Fig. 5) indicate that the fluorescence of the free enzyme (in the absence of gold nanoparticles) is significantly affected by the pH of the dispersing media. Free urease at its optimum working pH (i.e., 7.4) shows a peak at I_{max} 330 nm with emission intensity of 220 units. However, under slightly acidic or alkaline conditions, a noticeable quenching of the intrinsic fluorescence of urease could be observed. The extent of quenching is found to be relatively more prominent in acidic medium than the alkaline one. This could be ascribed to the unfolding of the enzyme under different pH conditions other than the optimum range,[32] thereby exposing the tryptophan and tyrosine residues.[34]

In the presence of the gold nanoparticles, however, a further decrease in the fluorescence intensity to values nearly close to zero for all the three urease nanoparticulate

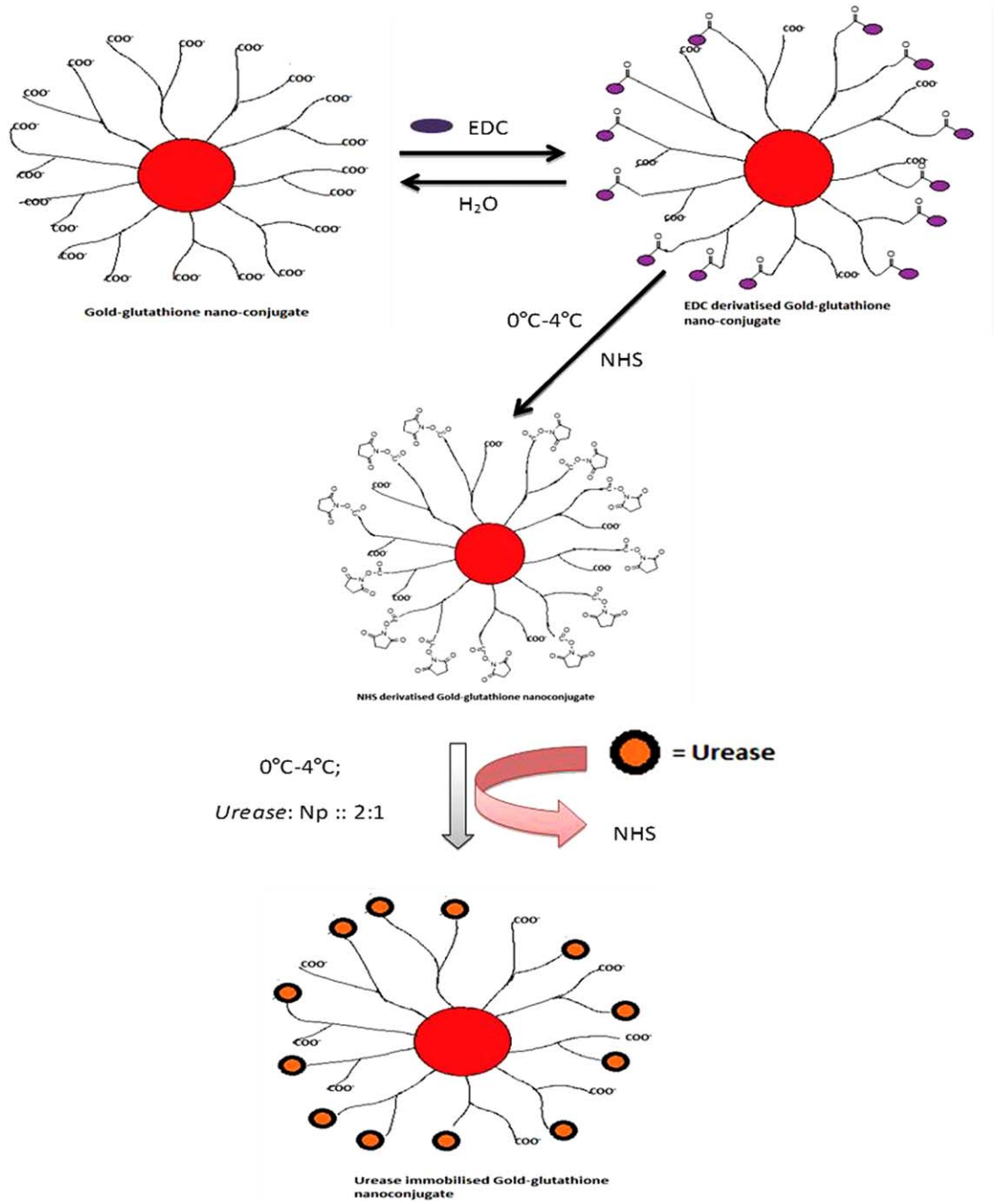

SCHEME 1. A schematic view of the covalent immobilization of urease on the surface of gold glutathione nano-conjugates. [Color figure can be viewed in the online issue, which is available at wileyonlinelibrary.com.]

suspensions (IM.U.4, IM.U.7, and IM.U.9) is observed. This inferred that a positive conjugation of urease to the surface of gold-glutathione nanoconjugates must have occurred at all the three pH values. Yet again, the quenching could be explained on the basis of the unfolding of urease upon immobilization which exposed the Tyr and Trp residues. Exposed amino acid residues can then transfer their resonance energy to the surface of nanoparticles resulting in subsequent quenching of their fluorescence.[35]

The emission curves of the supernatant (left after the separation of the immobilized enzyme pellet) at different pH values against the appropriate blank reference solutions [Fig. 6(a–c)] were also analyzed in order to quantify the immobilization extent.

The emission spectra of the blank solution as well as of the supernatant at pH 4.0 [Fig. 6(a)] showed complete pH induced fluorescence quenching and hence no conclusive data could be obtained from the results. On the other hand, supernatant at pH 7.4 [Fig. 6(b)] and pH 9.2 [Fig. 6(c)] gave a characteristic emission peak at λ_{max} value of 330 nm, (corresponding to the λ_{max} of free urease) with signal intensity quite lower than the intensity of their respective blanks.

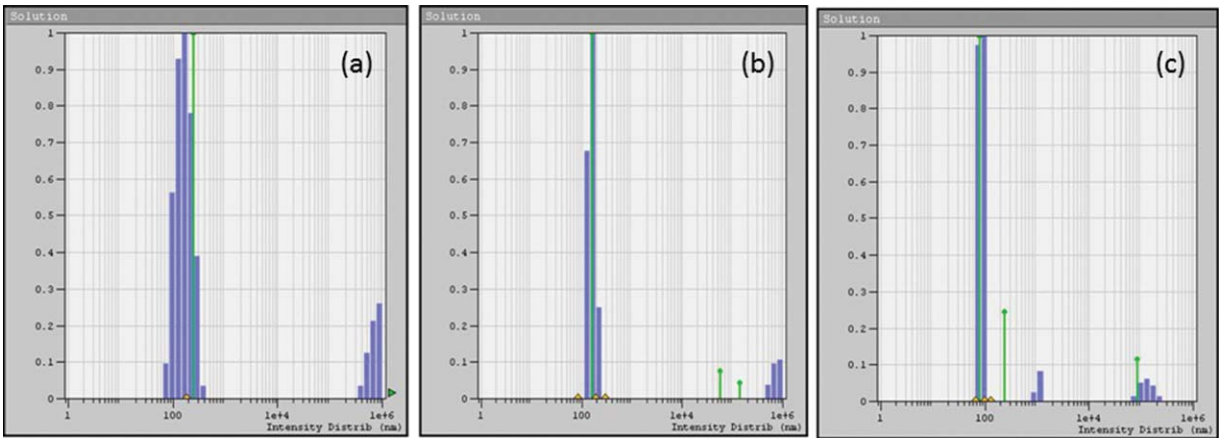

FIGURE 3. Size distribution plots (QELS data) of (a) IM.U.4 (b) IM.U.7 (c) IM.U.9. [Color figure can be viewed in the online issue, which is available at wileyonlinelibrary.com.]

Values of the emission intensities hence obtained (both for the free urease in blank reference solution as well as in the supernatant) were fitted in their respective standard calibration curves so as to determine the corresponding amount of urease (in milligrams) and consequently the percentage of immobilization (Table I).

Results indicate that maximum immobilization of urease on the surface of gold-glutathione nanoconjugates occurred at pH 7.4 with 98% percentage immobilization. A trivial decrease in the immobilization efficiency (to a value equivalent to 92%) is observed under slight alkaline conditions. However, no conclusive data could be obtained for the extent of immobilization at pH 4.0.

Thus spectroscopically, it could be established that an affirmative immobilization of urease on the surface of gold-glutathione nanoconjugates could occur at all the three pH values (4.0, 7.4, and 9.2) with variable extent of immobilization in each case. Simultaneously, it was also apparent that immobilization under any pH conditions led to significant changes in the microenvironment of enzyme. In order to substantiate these changes CD studies of the enzyme (before and after immobilization) at different pH values were carried out.

CD studies. CD spectra of the urease nanoparticulate suspensions (IM.U.4, IM.U.7, and IM.U.9) were analyzed and examined for the secondary structure content using the program CONTIN. However, in order to understand and recognize the conformational changes induced by immobilization, a prior knowledge regarding the pH induced conformational behavior was necessary.

CD spectra of the free urease at different pH values (Fig. 7) indicate that urease in its native form (at pH 7.4) exhibits two negative absorption bands at 208 and 220 nm, corresponding to α-helical and β-sheet content, respectively.[36] Under alkaline conditions (i.e., at pH 9.2) the intensity of the negative bands decreases slightly pointing toward a parallel decrease in α-helical and β-sheet content, however, at pH 4.0 a completely distorted CD spectrum with no distinct bands at 208 and 220 nm could be observed. Percentage secondary structure analysis authenticates the visual observations (Table II) by presenting similar results.

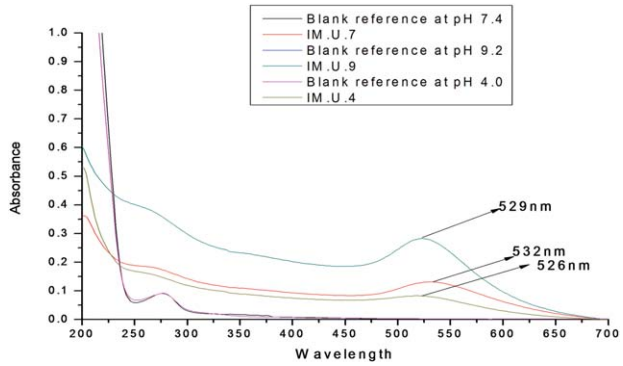

FIGURE 4. UV-Vis spectra of urease nano-particulate suspensions IM.U.4, IM.U.7 and IM.U.9 against respective standard blank reference solutions. [Color figure can be viewed in the online issue, which is available at wileyonlinelibrary.com.]

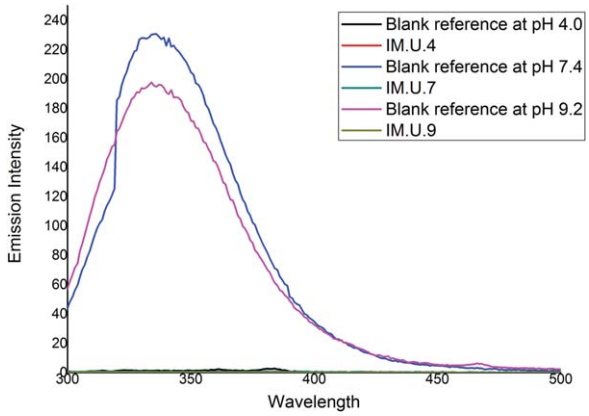

FIGURE 5. Emission curves of urease nano-particulate suspension IM.U.4, IM.U.7 and IM.U.9 against the blank reference solutions. [Color figure can be viewed in the online issue, which is available at wileyonlinelibrary.com.]

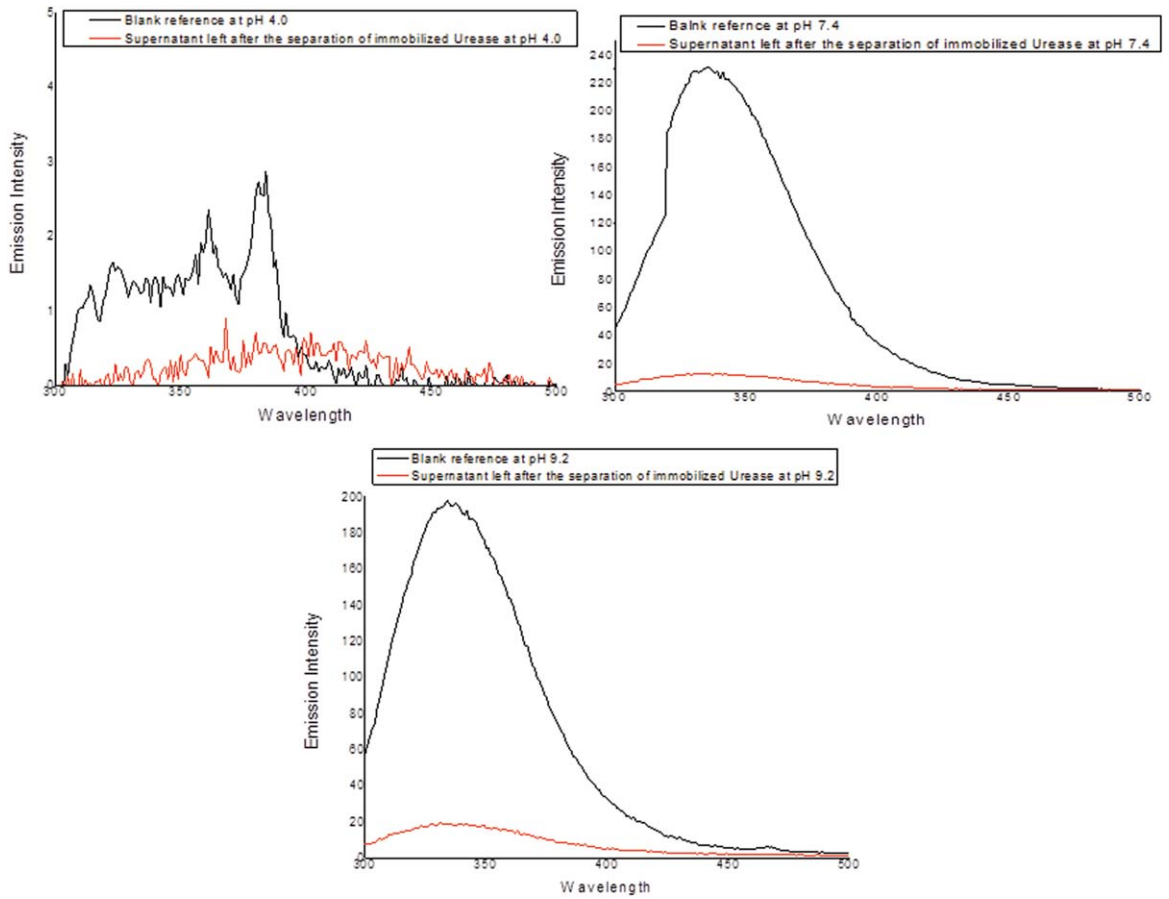

FIGURE 6. Emission curve of the supernatant left after the separation of immobilized urease against appropriate blank at (a) pH 4.0 (b) pH 7.4 (c) pH 9. [Color figure can be viewed in the online issue, which is available at wileyonlinelibrary.com.]

It is assumed that while slight reduction in the secondary structure could be attributed to an insignificant unfolding of the enzyme at pH 9.2, the drastic change, however, directs toward the possible dissociation of the hexameric urease into some active dissociation units in acidic environment.[32]

Keeping in mind the pH induced conformational effects, changes induced by immobilization of urease onto the surface of the gold-glutathione nanoconjugates at different pH values were also analyzed.

In general, CD spectra of the immobilized urease [Fig. 8(a–c)] against their respective blanks indicate that the secondary structure of the enzyme experienced drastic conformational changes (regardless of the pH induced changes) upon immobilization. In the acidic environment [Fig. 8(a)], not much visual changes in the CD spectra in comparison to its respective blank are observed (as pH induced changes itself were very significant). However, for IM.U.7 [Fig. 8(b)] and IM.U.9 [Fig. 8(c)], distinct and visible changes in the CD spectra of the immobilized enzyme with respect to their blank reference solution could be seen. Typically, the negative absorption bands at 208 and 220 nm (corresponding to the α-helical structure and β-sheet content, respectively) completely disappeared directing toward possible unfolding-refolding or dissociation-association phenomenon in the enzyme nanoparticulate suspensions at the pH values under consideration.[32]

Percentage secondary structure analysis (Table III), however, displayed slightly different scenario. It revealed that the immobilized enzyme retained most of its conformational integrity at pH 7.4 but exhibits drastic conformation changes

TABLE I. Tabulated View to Represent the Immobilization Percentage of Urease on the Surface of Gold-Glutathione Nano-Conjugates at Different pH Values

pH of the Dispersing Media	Concentration of the Urease in Blank (mg) C_i	Concentration of the Free Urease in Supernatant (mg)C_s	Net Concentration of Enzyme Immobilized (mg)$C_b = C_i - C_s$	Binding Efficiency ($C_b/C_i \times 100$) (%)
7.4	4.18	0.06	4.12	98.6
9.2	3.97	0.31	3.66	92.2

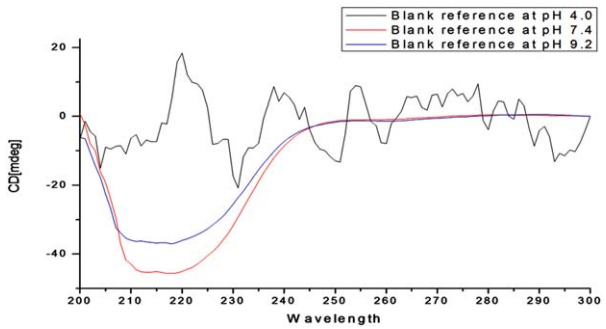

FIGURE 7. CD spectra of free urease in the blank reference solution at pH 4.0, 7.4 and 9.2. [Color figure can be viewed in the online issue, which is available at wileyonlinelibrary.com.]

under acidic and alkaline conditions. Hence it could be inferred that after immobilization where IM.U.7 resembled the native free urease conformation closely, IM.U.4 and IM.U.9 neither resembled their respective free counterparts, nor did they resemble the native enzyme at pH 7.4.

Bioactivity studies of urease nanoparticulate suspensions at different pH and thermal conditions

The conformational changes induced by the immobilization might affect the entire molecule or can only lead to the partial inactivation of the enzyme with its active site remaining intact. In order to evaluate these effects, bioassay of the urease nanoparticulate suspensions (IM.U.4, IM.U.7, and IM.U.9) against their respective blanks and with respect to the native enzyme (at is optimum conditions) was carried out. Bioactivity of urease (free as well as immobilized form) was investigated through the signature reaction of urease catalyzed hydrolysis of urea under different thermal conditions.

$$NH_2\text{–}CO\text{–}NH_2 + H_2O \rightarrow 2NH_3 + CO_2$$

The ammonium ions thus liberated were treated with Nessler's reagent that formed a brown colored precipitate. The amount of the brown precipitate (produced by the free as well as the immobilized urease under similar conditions of pH and temperature) was then determined gravimetrically so as to evaluate the percentage bioactivity. Since the maximum activity for the free enzyme is expected at pH 7.4 and temperature 60°C (optimum working conditions of urease) the activity of the enzyme at these conditions has been taken as reference (showing 100% results) and rest of the results are analyzed with respect to it.

TABLE II. Secondary Structure Content of Free Urease in Blank Reference Solution at Different pH Values

Sample	α-Helical Content (%)	β-Sheet Content (%)
Blank reference solution at pH 7.4	28.7	33.1
Blank reference solution at pH 9.2	25.4	29.0
Blank reference solution at pH 4.0	35.1	54.9

In order to substantiate the effect of immobilization on the bioactivity of urease, the effect of pH on its bioactivity under similar thermal conditions was investigated.

The bioactivity of free urease at different pH values (Fig. 9) clearly indicates that the enzyme exhibited maximum activity at pH 7.4 followed by the alkaline conditions (with 5%–8% loss in activity) and lastly the acidic medium (with 30%–40% loss in activity) at all the incubating temperatures. Such behavior can be easily explained on the basis of the pH induced conformational changes in free urease (Fig. 7 and Table II). The free enzyme maintained most of its conformation under alkaline conditions with respect to the native form, but encountered noteworthy conformational changes in the acidic medium.[36] Besides, it has also been observed that with the gradual increase in the incubation temperature from 0°C to 60°C, an equivalent increase in the activity of the free enzyme occurred under all pH conditions.

Keeping in view the above observations, a comparative analysis of the activity of the urease nanoparticulate suspensions (IM.U.4, IM.U.7, and IM.U.9) against their respective blanks and with respect to the native urease [Fig. 10(a–d)] was also carried out.

Percentage bioactivity studies reveal that immobilization under different pH conditions lead to differential activity of the immobilized urease. IM.U.4 [Fig. 10(a)] and IM.U.9 [Fig. 10(c)] indicates reduction in the enzyme activity whereas IM.U.7 [Fig. 10(b)] shows enhanced or equivalent bioactivity with respect to their respective blanks at all the temperatures. For IM.U.4, loss in the activity was not very prominent as merely a percentage decrease of 10%–15% was observed at different temperatures (with relatively improved activity at higher incubation temperatures viz. 37°C and 60°C). However, IM.U.9 displayed a percentage reduction of more than 70% in its activity. At pH 7.4 on the contrary, a percentage increase of about 10%–12% in the enzyme activity at 37°C and 60°C was observed pointing toward the synergistic effect of the immobilization on bioactivity.

The difference in the activity of the urease nanoparticulate suspension IM.U.4, IM.U.7, and IM.U.9 with respect to each other and against their respective blanks can be explained on the basis of changes in the conformation of the enzyme upon immobilization at different pH values. It has been observed that nanoparticulate suspension IM.U.7 did not show any significant changes in its conformation whereas IM.U.4 and IM.U.9 displayed noticeable conformational changes in comparison to their respective blanks after immobilization (Fig. 8 and Table III). As a consequence, IM.U.7 with negligible inactivation of the enzyme structure upon immobilization shows activity even greater than its free counterpart under certain thermal conditions. IM.U.4 on the other hand, though exhibits a secondary structure different from its native counterpart but since the loss in the activity of the urease after immobilization is not very significant, it can be easily postulated that immobilization

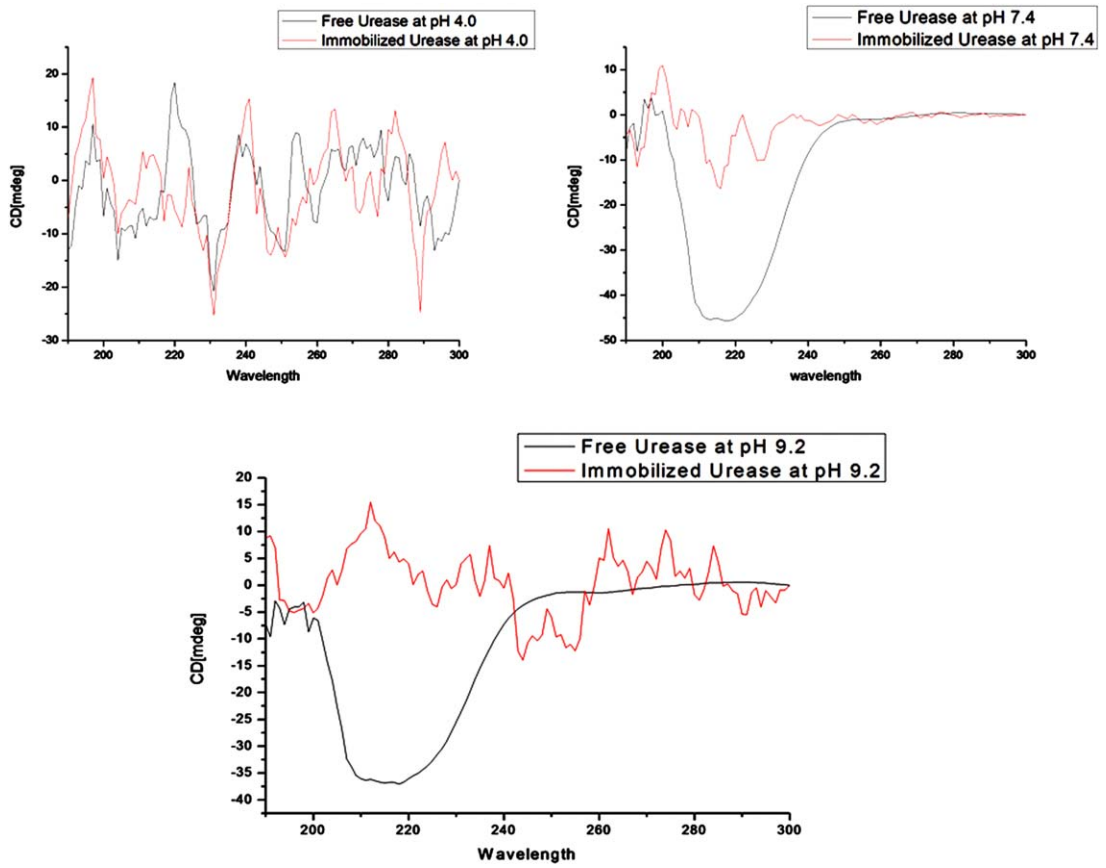

FIGURE 8. CD spectra of urease nano-particulate suspensions against the appropriate blank (a) IM.U.4 (b) IM.U.7 (c) IM.U.9. [Color figure can be viewed in the online issue, which is available at wileyonlinelibrary.com.]

resulted in partial inactivation of the enzyme with its active site remaining intact. In the case of IM.U.9, however, enzyme lost majority of its secondary structure after immobilization and also show highly diminished activity with respect to its blank. Hence it could be postulated that at pH 9.2, a completely denatured enzyme with inactivation of its entire structure was obtained after immobilization.

Furthermore, on comparing the bioactivity of enzyme nanoparticulate suspensions with that of the native enzyme [Fig. 10(d)] it was found that IM.U.7 showed an activity more than (or almost equivalent) the activity of reference (i.e., free enzyme at its optimum working condition). In contrast, IM.U.4 and IM.U.9 displayed significantly reduced activity with the percentage activity loss of 40%–60% and 80%–85%, respectively. While the reduction in the activity of IM.U.4 can be attributed to pH induced conformational changes, immobilization on the surface of gold nanoconjugates account for the reduced activity of IM.U.9.

Thus, the bioactivity analysis of the urease nanoparticulate suspensions indicate that immobilization of urease on the surface of the gold-glutathione nanoconjugates led to an enhanced overall activity of the enzyme when immobilized at the pH of 7.4. Immobilization under acidic medium also

TABLE III. Secondary Structure Content Analysis of the Urease Nanoparticulate Suspensions (IM.U.4, IM.U.7, and IM.U.9) Against the Appropriate Blanks

Sample Code	α-Helical Content (%)	β-Sheet Content (%)
Blank reference at pH 4.0	35.1	54.9
IM.U.4	61.9	38.1
Blank reference at pH 7.4	28.7	33.1
IM.U.7	27.8	34.3
Blank reference at pH 9.2	25.4	29.0
IM.U.9	0.0	39.02

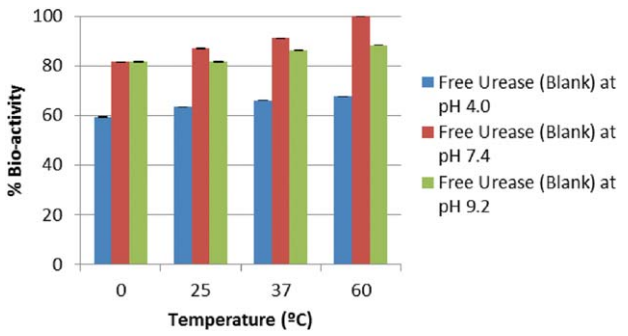

FIGURE 9. Graphical illustration of the relative bio-activity of the free urease under different pH and thermal conditions. [Color figure can be viewed in the online issue, which is available at wileyonlinelibrary.com.]

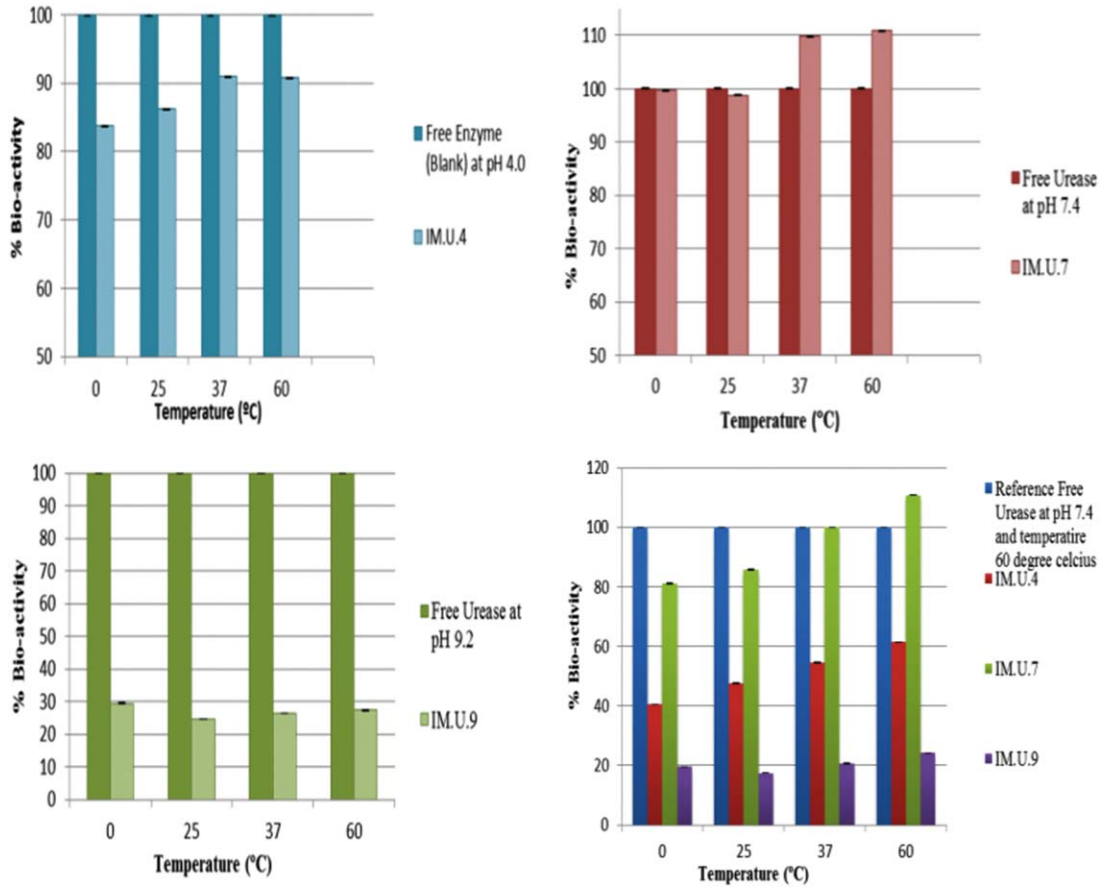

FIGURE 10. Graphical illustration of the bio-activity of the urease nano-particulate suspensions at different temperatures (a) IM.U.4 against its blank (b) IM.U.7 against its blank (c) IM.U.9 against its blank (d) IM.U.4, IM.U.7 and IM.U.9 against native urease. [Color figure can be viewed in the online issue, which is available at wileyonlinelibrary.com.]

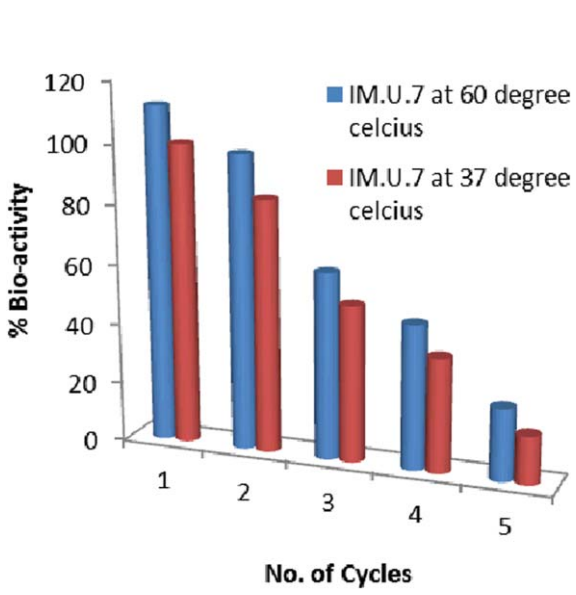

FIGURE 11. Graphical illustration of recyclability studies of IM.U.7. [Color figure can be viewed in the online issue, which is available at wileyonlinelibrary.com.]

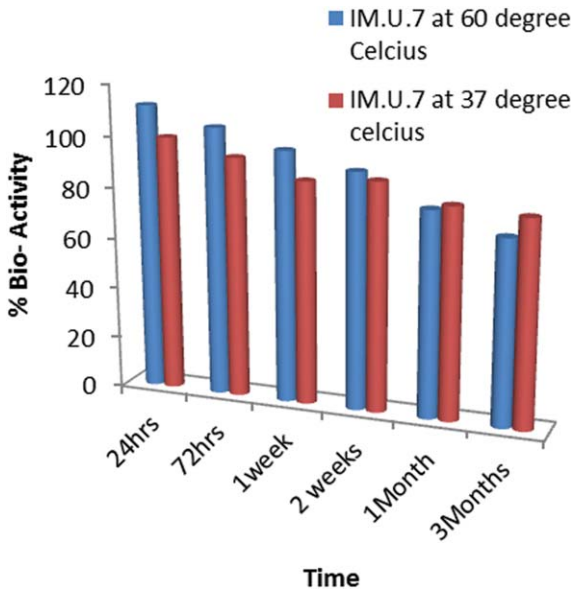

FIGURE 12. Shelf life studies of urease nano-particulate suspension IM.U.7. [Color figure can be viewed in the online issue, which is available at wileyonlinelibrary.com.]

resulted in the retained activity of the enzyme with respect to its free counterpart. However, immobilization of urease in alkaline conditions brought about almost complete loss of its activity at all the thermal conditions. As a consequence, IM.U.9 can be completely discarded as far as its application in the biomedical field is concerned.

Recyclability studies of urease nanoparticulate suspension

Based upon the promising results obtained from the bioactivity studies of urease nanoparticulate suspension IM.U.7, the recyclability studies of the same in terms of its percentage bioactivity (after repeated cycles of hydrolysis of urea) at temperatures of 37°C and 60°C, respectively, were carried out.

It was found that IM.U.7 worked efficiently up till four cycles of its use with the percentage activity of more than 50% (Fig. 11). However, at the fifth cycle, a significant loss in its activity with a percentage reduction of around 80% could be observed. The noticeable reduction in the enzyme activity can be attributed to the possible saturation of the active site of the enzyme with every passing cycle resulting in the corresponding decrease in the rate of hydrolysis of urea and hence the reduced percentage bioactivity.

Shelf-life studies of urease nanoparticulate suspension

Shelf life of the urease nanoparticulate suspension IM.U.7 was also studied in order to further explore the advantages offered by the immobilization approach. Shelf-life studies were carried out in terms of percentage bioactivity of the enzyme (stored at cold temperatures) at different time intervals at the temperatures of 37°C and 60°C.

Results revealed that the nanoparticulate suspension IM.U.7 (Fig. 12) could be stored effectively in its immobilized form for a time period of about 3 months with more than 85% and 80% of its bioactivity retained at temperature of 37°C and 60°C, respectively.

CONCLUSION

Our group has reported the use of nanoparticles in biomedical applications[37,38] and catalysis[39–52] in the past. Here we have demonstrated the use of gold nanoparticles for immobilization of urease, a technique that could potentially be used to immobilize other relevant proteins and bioactive peptides.[53–55] The surface of the gold-glutathione nanoconjugates designed with the aim of easy and efficient interaction with a range of biologically relevant molecules has been employed for the covalent immobilization of the enzyme urease. Immobilization has been attempted at different pH conditions so as to elucidate the effect of both pH and immobilization on the conformation and subsequent bioactivity of the enzyme. Spectroscopic studies (absorption and emission spectroscopy) established that successful immobilization of urease on the solid nanosupport could occur at all the chosen pH values with an immobilization efficiency of around 98% at pH 7.4 and 92% at pH 9.2, respectively. CD studies have been employed to gain a deeper insight into the conformational behavior of the enzyme before and after immobilization at different pH values. Results revealed that immobilization at the pH value of 7.4 led to minimum conformational changes in the structure of the enzyme. The bioactivity of the urease nanoparticulate suspensions has been found to be in close correlation with the conformational changes in the structure of the enzyme. As a consequence, IM.U.7 gave the most promising results in terms of its percentage bioactivity in comparison to IM.U.4 and IM.U.9. It has also been realized that the reduction in the bioactivity of IM.U.4 was mainly because of the pH induced conformational changes whereas the lower bioactivity of IM.U.9 was largely due to the conformational changes induced by the immobilization. Thermal stability of the immobilized enzyme suspensions has also been evaluated which showed an extended stability of the immobilized enzyme at temperatures of 37°C–60°C in comparison to only 60°C for the free native part. Possible recyclability and extended shelf life of the urease nanoparticulate suspensions against its native counterpart further added to the advantages offered by the immobilization approach.

Therefore, immobilized urease showed better results than the native enzyme (in terms of activity, pH, and thermal stability or recyclability) and it could be concluded that they can be safely developed as biosensors, for immunoassays and as *in vivo* diagnostic tools in the future. Moreover, the gold-based nanovehicle could be seen as an effective immobilization surface for a large number of enzymes and other biologically important moieties (as it could broaden the application of the enzyme by either improving its activity and stability or by enhancing its shelf life and recyclability) in the future.

REFERENCES

1. Lynch I, Dawson KA. Protein-nanoparticle interactions. Nanotoday 2008;3:40–47.
2. Husain Q. β Galactosidase and their potential applications. Crit Rev Biotechnol 2010;30:41–62.
3. Lei C, Shin Y, Liu J, Ackerman EJ. Entrapping enzyme in a functionalized nanoporous support. J Am Chem Soc 2002;124:11242–11243.
4. Tischer W, Wedekind F. Immobilized enzymes: Methods and applications. Top Curr Chem 1999;200:95–126.
5. Wang, P. Nanoscale biocatalyst systems. Curr Opin Biotechnol 2006;17:574–579.
6. Alonso N, Lopez-Callego F, Betancor L, Hidalgo A, Mateo C, Guisan JM, Fernandez Lafuente R. Immobilization and stabilization of glutaryl acylase on aminated sepabeads supports by the glutaraldehyde crosslinking method. J Mol Catal B: Enzym 2005;35:57–61.
7. Kondo A, Murakami F, Kawagoe M, Higashitani K. Kinetics and circular dichroism of enzymes adsorbed on ultrafine silica particles. Appl Microbiol Biotechnol 1993;39:726–731.
8. Hamerska-Dudra A, Bryjak J, Trochimczuk AW. Novel method of enzymes stabilization on crosslinked thermosensitive carriers. Enzym Microb Technol 2006;38:921–925.
9. Lopez-Callego F, Betancor L, Hidalgo A, Dellamora-Ortiz G, Mateo C, Fernandez-Lafuente R, Guisan JM. Stabilization of different alcohol oxidases via immobilization and post immobilization technique. Enzym Microb Technol 2007;40:278–284.
10. De Temino, DMR, Hartmeier W, Ansorge-Schumacher MB. Entrapment of the alcohol dehydrogenase from Lactobacillus kefir in polyvinyl alcohol for the synthesis of chiral hydrophilic alcohols in organic solvents. Enzym Microb Technol 2005;36:3–9.
11. Kim J, Grate JW, Wang P. Nanostructures for enzyme stabilization. Chem Eng Sci 2006;61:1017–1026.

12. Zhao H-Z, Sun J-J, Song J, Yang Q-Z. Direct electron transfer and conformational changes of glucose oxidase on carbon nanotubes-based electrodes. Carbon 2010;48:1508–1514.
13. Ma S, Mu J, Qu Y, Jiang L. Effect of refluxed silver nanoparticles on inhibition and enhancement of enzymatic activity of glucose oxidase. Colloids Surf A: Physicochem Eng Aspects 2009;345:101–105.
14. Mitchell DT, Lee SB, Trofin L, Li N, Nevanen TK, Soderlund H, Martin CR. Smart nanotubes for bioseparations and biocatalysis. J Am Chem Soc 2002;124:11864–11865.
15. Crespilho FN, Ghica ME, Florescu M, Nart FC, Oliveira Jr ON, Brett CMA. A strategy for enzyme immobilization on layer-by-layer dendrimer-gold nanoparticle electrocatalytic membrane incorporating redox mediator. Electrochem Commun 2006;8: 1665–1670.
16. Lia Y, Schluesenerb HJ, Xu S. Gold nanoparticle-based biosensors. Gold Bull 2010;43:29–41.
17. Xu J, Zeng F, Wu S, Liu X, Hou C, Tong Z. Gold nanoparticles bound on microgel particles and their application as an enzyme support. Nanotechnology 2007;18:265–273.
18. Lin J, Zhou W, Kumbhar A, Wiemann J, Fang J, Carpentier EE, O'Connor CJ. Gold-coated iron (Fe@Au) nanoparticles: Synthesis, characterization and magnetic field inducedself-assembly. Solid State Chem 2001;159:26–31.
19. Vertegel AA, Siegel RW, Dordick JS. Silica nanoparticle size influences the structure and enzymatic activity of adsorded lysozyme. Langmuir 2004;20:6800–6807.
20. Pandey P, Singh SP, Arya SK, Gupta V, Datta M, Singh S, Malhotra BD. Application of thiolated gold nanoparticles for enhancement of glucose oxidase activity. Langmuir 2007;23:3333–3337.
21. Petkova1 GA, Záruba1 K, Žvátora1 P, Král V. Gold and silver nanoparticles for biomolecule immobilization and enzymatic catalysis. Nanoscale Res Lett 2012;7:287–297.
22. Pozniak G, Krajewska B, Trochimczuk W. Urease immobilized on modified polysulphone membrane: Preparation and properties. Biomaterials 1995;16:129–134.
23. Chellapandian M, Krishnan MRV. Chitosan-poly (glycidyl methacrylate) copolymer for immobilization of urease. Process Biochem 1998;33:595–600.
24. Sahoo B, Sahu SK, Pramanik P. A novel method for the immobilization of urease on phosphonate grafted iron oxide nanoparticle. J Mol Catal B: Enzymatic 2011;69:95–102.
25. Laska J, Wlodarczyk J, Zaborska W. Polyaniline as a support for urease immobilization. J Mol Catal B: Enzymatic 1999;6:549–553.
26. Senel M, Coskun A, Abasıyanık MF, Bozkurt A. Immobilization of urease in poly(1-vinyl imidazole)/poly(acrylic acid) network. Chem Pap 2010;64:1–7.
27. Chen JP, Chiu SH. A poly(N-isopropylacrylamide-co-N-acryloxysuccinimide-co-2-hydroxyethyl methacrylate) composite hydrogel membrane for urease immobilization to enhance urea hydrolysis rate by temperature swing. Enzym Microb Technol 2000;26:359–367.
28. Liang ZP, Feng YQ, Meng SX, Liang ZY. Preparation and properties of urease immobilized onto glutaraldehyde cross-linked chitosan beads. Chin Chem Lett 2005;16:135–138.
29. Pithawala K, Mishra N, Bahadur A. Immobilization of urease in alginate, paraffin and lac. J Serb Chem Soc 2010;75:175–183.
30. Rao MS, Chellapandian M, Krishnan MRV. Immobilization of urease on gelatin-poly (HEMA) copolymer preparation and characterization. Bioprocess Eng 1995;13:211–214.
31. Mahmoudi M, Lynch I, Ejtehadi RM, Monopoli MP, Bombelli FB, Laurent S. Protein-nanoparticle interactions: Opportunities and challenges. Chem Rev 2011;111:5610–5637.
32. Omar S, Beauregard M. Dissociation and unfolding of jack bean urease studied by fluorescence emission spectroscopy. J Biotechnol 1995;39:221–228.
33. Zhang HM, Zhang GC, Wang YQ. The interaction of chromium(VI) with urease in solution. Biol Trace Elem Res 2011;41:53–64.
34. Lakowicz JR. Principles of Fluorescence Spectroscopy, 3rd ed. Baltimore, Maryland: University of Maryland School of Medicine.
35. Dulkeith E, Morteani AC, Niedereichholz T, Klar TA, Feldmann J, Levi SA, van Veggel FCJM, Reinhoudt DN, Möller M, Gittins DI. Fluorescence quenching of dye molecules near gold nanoparticles: Radiative and nonradiative effects. Phys Rev Lett 2002;89: 2030021–2030024.
36. Jana S, Chaudhuri TK, Deb JK. Effects of guanidine hydrochloride on the conformation and enzyme activity of streptomycin adenylyltransferase monitored by circular dichroism and fluorescence spectroscopy. Biochemistry (Moscow) 2006;71:1230–1237.
37. Aerry S, De A, Saxena A, Majumdar D, Mozumdar S. Synthesis and characterization of thermoresponsive copolymers for drug delivery. J Biomed Mater Res Part A 2013;101:2015–2026.
38. Garg S, De A, Nandi T, Mozumdar S. Synthesis of a smart gold nano-vehicle for liver specific drug delivery. AAPS PharmSciTech 2013;14:1219–1226.
39. Kumar A, Aerry S, Saxena A, De A, Mozumdar S. Copper nanoparticulates in Guar-gum: A recyclable catalytic system for the Huisgen [3+ 2]-cycloaddition of azides and alkynes without additives under ambient conditions. Green Chem 2012;14:1298–1301.
40. Kumar A, Dewan M, De A, Saxena A, Aerry S, Mozumdar S. Aldol condensation in PEG-400 catalyzed by recyclable l-proline supported on nano gold surface. RSC Adv 2013;3:603–607.
41. Kumar A, Saxena A, De A, Shankar R, Mozumdar S. Facile synthesis of size-tunable copper and copper oxide nanoparticles using reverse microemulsions. RSC Adv 2013;3:5015–5021.
42. Dewan M, Kumar A, Saxena A, De A, Mozumdar S. Using hydrophilic ionic liquid,[bmim] BF4–ethylene glycol system as a novel media for the rapid synthesis of copper nanoparticles. PLoS One 2012;7:e29131.
43. Dewan M, Kumar A, Saxena A, De A, Mozumdar S. Biginelli reaction catalyzed by copper nanoparticles. PLoS One 2012;7:e43078.
44. Dewan M, Kumar A, Saxena A, De A, Mozumdar S. Molecular iodine in [bmim][BF4]: A highly efficient green catalytic system for one-pot synthesis of 1, 3-oxathiolan-5-one. Tetrahedron Lett 2010;51:6108–6110.
45. Kumar A, Saxena A, Dewan M, De A, Mozumdar S. Recyclable nanoparticulate copper mediated synthesis of naphthoxazinones in PEG-400: A green approach. Tetrahedron Lett 2011;52:4835–4839.
46. Kumar A, Dewan M, Saxena A, De A, Mozumdar S. Knoevenagel condensation catalyzed by chemo-selective Ni-nanoparticles in neutral medium. Catal Commun 2010;11:679–683.
47. Kumar A, Saxena A, De A, Mozumdar S. Ni-nanoparticles: An efficient catalyst for the synthesis of quinoxalines. Catal Commun 2008;9:778–784.
48. Kumar A, Kumar S, Saxena A, De A, Mozumdar S. Selective protection of carbonyl compounds over nano-sized nickel catalysts. Catal Lett 2008;122:98–105.
49. Kumar A, Singh P, Saxena A, De A, Chandra R, Mozumdar S. Nano-sized copper as an efficient catalyst for one pot three component synthesis of thiazolidine-2, 4-dione derivatives. Catal Commun 2008;10:17–22.
50. Kumar A, De A, Saxena A, Mozumdar S. Environmentally benign synthesis of positively charged, ultra-low sized colloidal gold in universal solvent. Adv Nat Sci: Nanosci Nanotechnol 2014;5: 025017.
51. Kumar A, Saxena A, De A, Shankar R, Mozumdar S. Controlled synthesis of size-tunable nickel and nickel oxide nanoparticles using water-in-oil microemulsions. Adv Nat Sci: Nanosci Nanotechnol 2013;4:025009.
52. Aerry S, Kumar A, Saxena A, De A, Mozumdar S. Chemoselective acetylation of amines and thiols using monodispersed Ni-nanoparticles. Green Chem Lett Rev 2013;6:183–188.
53. De A, DiMarchi RD. Synthesis and characterization of ester-based prodrugs of glucagon-like peptide 1. Pept Sci 2010;94:448–456.
54. De A, DiMarchi RD. Investigation of the feasibility of an amide-based prodrug under physiological conditions. Int J Pept Res Ther 2008;14:255–262.
55. De A, DiMarchi R. Synthesis and characterization of peptide hormone-based prodrugs. Biopolymers 2009;92:324–325.